Developmental Cell
Article

Lipoprotein-Heparan Sulfate Interactions in the Hh Pathway

Christina Eugster,[1] Daniela Panáková,[1,2] Ali Mahmoud,[1] and Suzanne Eaton[1,*]
[1] Max Planck Institute of Molecular Cell Biology and Genetics, Pfotenhauerstrasse-108, 01307 Dresden, Germany
[2] Present address: Cardiovascular Research Center, Massachusetts General Hospital, 149 13th Street, 149-4201, Charlestown, MA 02129, USA.
*Correspondence: eaton@mpi-cbg.de
DOI 10.1016/j.devcel.2007.04.019

SUMMARY

The *Drosophila* lipoprotein particle, Lipophorin, bears lipid-linked morphogens on its surface and is required for long-range signaling activity of Wingless and Hedgehog. Heparan sulfate proteoglycans are also critical for trafficking and signaling of these morphogens. Here we show that Lipophorin interacts with the heparan sulfate moieties of the glypicans Dally and Dally-like. Membrane-associated glypicans can recruit Lipophorin to disc tissue, and remain associated with these particles after they are released from the membrane by cleavage of their gpi anchors. The released form of Dally colocalizes with Patched, Hedgehog, and Lipophorin in endosomes and increases Hedgehog signaling efficiency without affecting its distribution. These data suggest that heparan sulfate proteoglycans may influence lipid-linked morphogen signaling, at least in part, by binding to Lipophorin. They further suggest that the complement of proteins present on lipoprotein particles can regulate the activity of morphogens.

INTRODUCTION

Controlling the spread and signaling of secreted morphogens is of critical importance for pattern formation during development (Ashe, 2005; Ashe and Briscoe, 2006; Day and Lawrence, 2000; Eaton, 2006; Gurdon and Bourillot, 2001; Ruiz i Altaba et al., 2003; Vincent and Dubois, 2002). Morphogens of the Wnt and Hedgehog families undergo covalent lipid modification (Pepinsky et al., 1998; Porter et al., 1996; Willert et al., 2003); these lipid moieties are essential for normal trafficking and signaling (Callejo et al., 2006; Chamoun et al., 2001; Gallet et al., 2003, 2006; Lewis et al., 2001; Pepinsky et al., 1998; Willert et al., 2003). The cell biological mechanisms they influence are not completely understood. We have recently shown that the lipid-linked morphogens Wingless (Wg) and Hedgehog (Hh) can be released from the plasma membrane on the *Drosophila* lipoprotein Lipophorin, and that Lipophorin is important for their long-range but not short-range signaling activity (Panáková et al., 2005). How might Lipophorin association influence morphogen signaling activity? One function of Lipophorin may be to mobilize otherwise membrane-bound molecules for long-range movement. Furthermore, a variety of gpi-linked proteins are also found on these particles, raising the possibility that morphogen signaling could be subject to additional regulation by other particle-associated proteins.

Heparan sulfate proteoglycans (HSPGs) are also essential for normal trafficking and signaling of morphogens. Sterol-modified Hh cannot accumulate in or move through tissue that does not synthesize heparan sulfate (HS). In contrast, truncated Hh that cannot be sterol modified spreads freely through tissue missing HS. The effects of HS on the Hh pathway are mediated at least in part by the glypicans Dally and Dally-like (Dlp) (Baeg et al., 2004; Franch-Marro et al., 2005; Han et al., 2004b, 2005; Kreuger et al., 2004). Whereas Dlp is required for Hh signaling in S2 cells, it appears to act redundantly with Dally in imaginal discs. Only clones of cells mutant for both *dally* and *dlp* show autonomous reduction in Hh signaling (Han et al., 2004b).

While autonomous functions of Dally and Dlp are presumably exerted by membrane-linked forms of the proteins, Dlp can also be shed from the plasma membrane. Notum, an enzyme in the α/β hydrolase family, removes the gpi anchor from Dlp expressed in S2 cells, releasing the protein into the supernatant (Kreuger et al., 2004). Whether Dally can be detached from its gpi anchor by Notum or other enzymes is unresolved (Han et al., 2004b; Kreuger et al., 2004). Some gpi-anchored proteins are released from cell membranes by associating with lipoprotein via their lipid anchors (Panáková et al., 2005), suggesting yet another mechanism for glypican shedding. It is not yet clear how and to what extent shedding occurs in vivo. Furthermore, specific roles for shed glypicans would be difficult to detect genetically because mutant clones have access to released glypicans produced by wild-type tissue.

Here we examine the relationship between glypicans and Lipophorin in the Hh pathway. We find that Lipophorin binds to the HS moieties of glypicans and can be recruited to disc tissue by these proteins. Lipophorin remains associated with glypicans when they are released from the plasma membrane by gpi removal. The released form of Dally is found in endosomes containing Lipophorin, Hh,

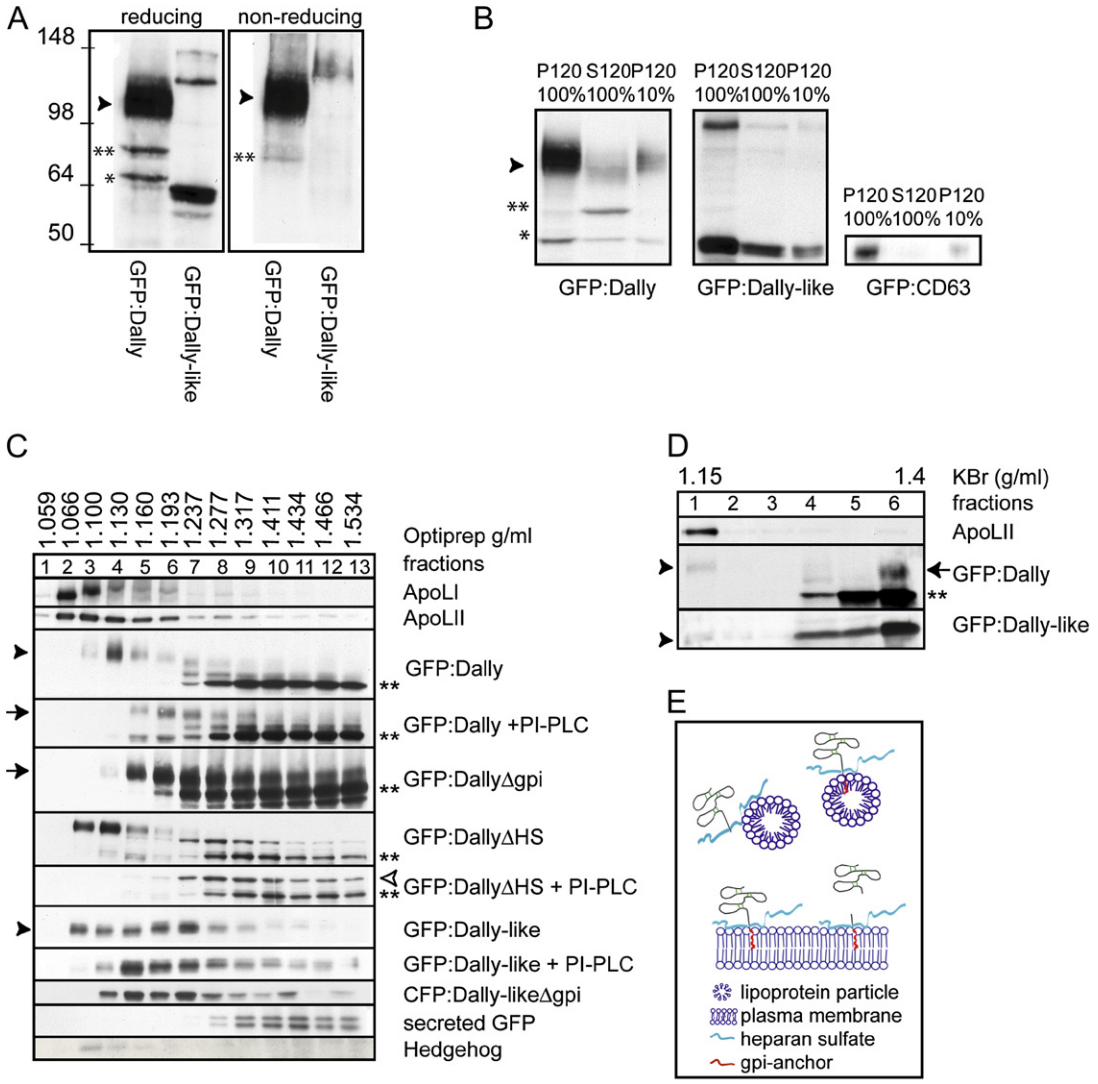

Figure 1. Dally and Dlp Are Released from Membranes

(A) Extracts of imaginal discs expressing either GFP:Dally or GFP:Dlp in the posterior compartment electrophoresed under reducing or nonreducing conditions and probed with anti-GFP.

(B) Western blots of 120,000 × g supernatants (S120s) and pellets (P120s) of GFP:CD63-, GFP:Dally-, or GFP:Dlp-expressing disc extracts, probed with anti-GFP. A fraction of GFP:Dally and GFP:Dlp remains in S120 under conditions that pellet membrane proteins (GFP:CD63).

(C) Optiprep density gradient fractions of S120s from larvae expressing indicated GFP fusion proteins in imaginal discs. Gradients are probed with anti-GFP or anti-Hh. Even non-gpi-linked glypicans (arrowheads) fractionate with Lipophorin (ApoLII).

(D) Western blots of KBr gradient fractions from S120 of GFP:Dally- or GFP:Dlp-expressing discs; 10%–20% of released glypicans cofractionate with Lipophorin. In (A)–(D) Asterisks indicate proteolytic cleavage products.

(E) Glypican isoforms.

and the Hh receptor Patched (Ptc) and increases Hh signaling efficiency.

RESULTS

Processing of Glypicans by Imaginal Disc Cells

To study the distribution and processing of Dally and Dlp in disc epithelia, we constructed GFP fusions of both wild-type and mutant forms and expressed them in discs using the GAL4UAS system. Western blotting against GFP shows that GFP:Dally exists in both full-length (arrowheads in Figure 1A) and proteolytically cleaved forms (asterisks). The full-length form of GFP:Dally migrates between 110 and 125 kD, larger than the 95 kD predicted for the core protein. Both gpi addition and heparan sulfate modification contribute to this increase in apparent

molecular weight. Mutating heparan sulfate addition sites decreases the molecular weight of GFP:Dally by approximately 10–15 kD (see Figure S1A in the Supplemental Data available with this article online). Removing the gpi anchor either genetically (Figure S1A) or by PI-PLC treatment (Figure S1B) also decreases the apparent molecular weight by 10–15 kD. As the gpi anchor is less than 1 kD, lipid modification may change the conformation of the protein. Removing both HS addition sites and the gpi anchor from GFP:Dally produces a single sharp band with the predicted molecular weight of the core protein (Figure S1B, empty arrowhead).

A small fraction of GFP:Dally is proteolytically processed to separate the N-terminal cysteine-rich domain from the HS-modified and gpi-anchored C-terminal domain (Figures 1A and 1E). Anti-GFP antibodies detect two N-terminal fragments (asterisks in Figure 1A). The smaller of the two cleaved forms of GFP:Dally (Figure 1A, single asterisk) disappears when gels are run in the absence of reducing agent, indicating it is normally attached to the rest of the protein via disulfide bonds.

To test what fraction of GFP:Dally was gpi linked, we examined its behavior upon phase separation in solutions of TX-114. Full-length GFP:Dally partitions into both aqueous and detergent phases of TX-114, suggesting that it is released in both gpi-modified and unmodified forms (Figure S1C). Consistent with this, the protein present in the aqueous phase is of slightly faster mobility, similar to that of non-gpi-modifiable GFP:DallyΔgpi.

GFP:Dlp is also cleaved into two fragments that remain associated via disulfide bonds, consistent with previous studies of glypican-3 (De Cat et al., 2003). On reducing gels, most GFP:Dlp migrates between 61 and 63 kD; in the absence of reducing agent, its apparent molecular weight is between 120 and 135 kD, consistent with the size of the core protein plus heparan sulfate moieties (Figure 1A).

Glypicans Are Shed by Imaginal Disc Cells

To ask which glypican isoforms were membrane associated, we performed differential centrifugation on homogenates of GFP:Dlp- and GFP:Dally-expressing discs. Spinning at 120,000 × g for 3 hr efficiently pellets membrane proteins such as GFP:CD63 (Figure 1B). While approximately 90% of full-length GFP:Dally is in the membrane pellet (P120) under these conditions, 10% remains in the supernatant (S120). In contrast, the majority of the 75 kD cleavage product corresponding to the released cysteine-rich domain remains in the supernatant, confirming it is not membrane associated (Figure 1B). Similarly, 80% of GFP:Dlp is membrane associated, whereas 20% remains in the supernatant (Figure 1B). Thus, Dally and Dlp exist in membrane-associated and released forms in imaginal discs.

Glypicans Bind to Lipoprotein Particles via Either the Gpi Anchor or Heparan Sulfate

Gpi-linked proteins can be shed from membranes by multiple mechanisms. The lipid anchor can be removed by proteases or by lipases. Also, binding of the gpi anchor to lipoprotein particles can allow release of these proteins with their lipid anchors intact (Panáková et al., 2005). To test whether shed glypicans might associate with low-density particles or whether they were released in soluble form, we compared fractionation of released GFP:Dally and GFP:Dlp to that of Lipophorin particles in isopycnic density gradients of either KBr or Optiprep. In Optiprep gradients, soluble proteins like secreted GFP, or the N-terminal fragment of GFP:Dally (asterisks), move to high-density fractions 9–13 (Figure 1C). In contrast, western blotting with antibodies to the nonexchangeable Apolipophorins I and II (ApoLI, ApoLII) shows that most Lipophorin particles are present in lower-density fractions 2–6 (Figure 1C). Within this region, lipoproteins of different densities contain different proportions of ApoLII and ApoLI, and ApoLI in fractions 4–6 has a slower apparent mobility, suggesting it may be modified more extensively. Thus, different Optiprep fractions contain particles of specific densities and compositions.

The full-length non-membrane-associated forms of both GFP:Dally and GFP:Dlp comigrate almost entirely with Lipophorin in Optiprep gradients (Figure 1C, arrowheads). Interestingly, only 10%–20% of GFP:Dally and GFP:Dlp cofractionates with Lipophorin when gradients are run in KBr instead of Optiprep (Figure 1D). Optiprep gradients are iso-osmotic; in contrast, the salt concentration in KBr gradients starts at about 2 M. These data suggest that shed glypicans associate with lipoprotein particles by two different mechanisms, only one of which is resistant to high salt.

As hydrophobic interactions mediated by the gpi anchor should be unaffected by salt concentration, we considered the possibility that ionic interactions might allow non-gpi-anchored Dally to fractionate with Lipophorin in Optiprep gradients. Consistent with this, the mobility of GFP:Dally in high-density, soluble fractions of KBr gradients resembles that of the non-gpi-anchored form (Figure 1D, arrow). Furthermore, removing the gpi anchor either genetically or using PI-PLC completely prevents the migration of GFP:Dally to the low-density fractions of KBr gradients (Figure S1D), but only slightly affects its fractionation in Optiprep gradients (Figure 1C, arrows). Thus, non-gpi-modified glypicans can associate with Lipophorin particles under physiological salt conditions, but salt-stable binding requires the gpi anchor.

Vertebrate lipoprotein particles bind to heparan sulfate (Kolset and Salmivirta, 1999; Wilsie et al., 2005; Wilsie and Orlando, 2003). Therefore, we suspected that heparan sulfate might mediate binding of Dally to Lipophorin in the absence of its gpi anchor. To investigate this, we examined fractionation of GFP:Dally missing either HS addition sites (GFP:DallyΔHS) or both HS addition sites and the gpi anchor. Whereas removing only HS did not compromise cofractionation with Lipophorin (Figure 1C, sixth panel), removing both HS and the gpi anchor caused GFP:Dally to shift almost entirely to high-density fractions with soluble proteins (Figure 1C, open arrowhead). Thus, GFP:Dally can

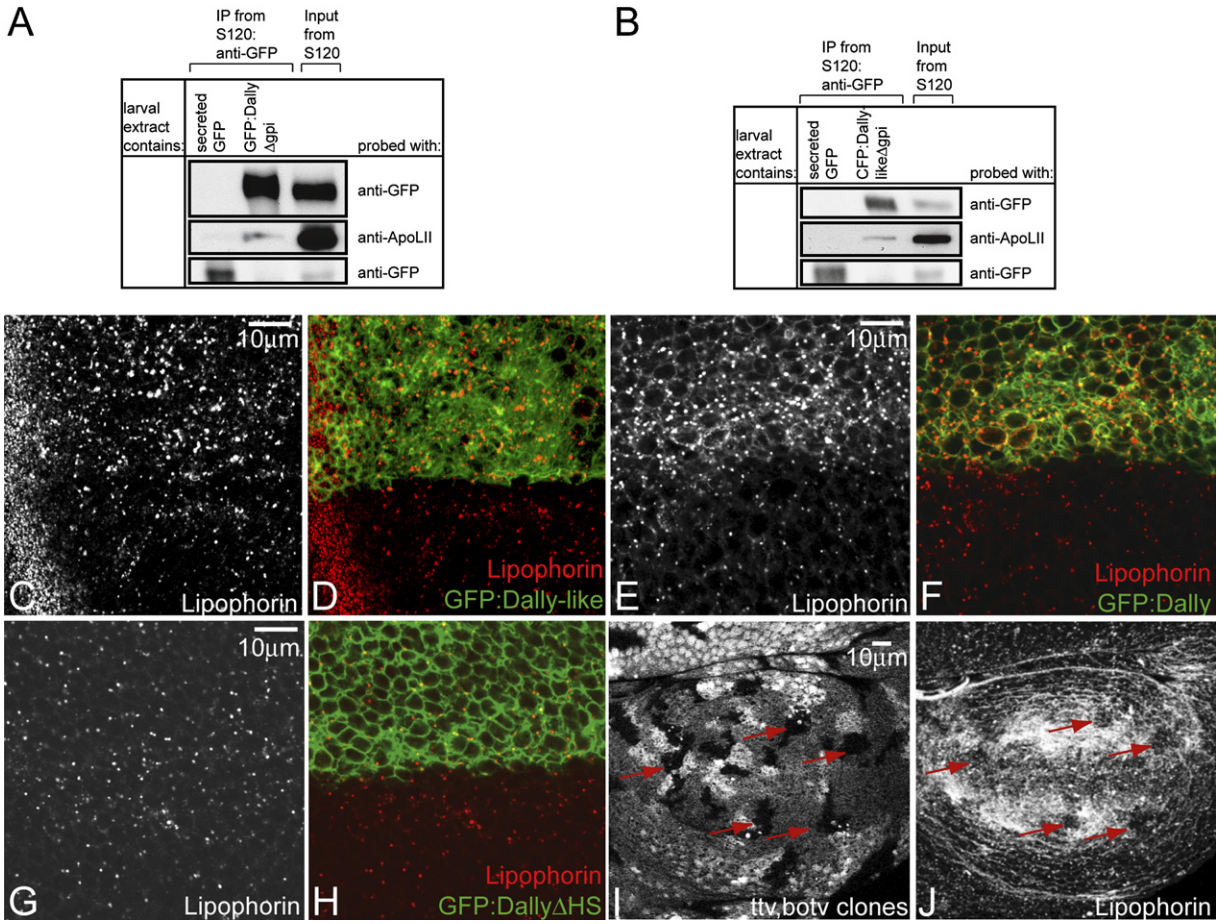

Figure 2. GPI-Independent Glypican-Lipophorin Interaction

(A and B) Anti-GFP immunoprecipitates from disc S120s expressing GFP:DallyΔgpi, CFP:DlpΔgpi, or secreted GFP blotted and probed with anti-GFP or anti-Lipophorin (ApoLII). Lipophorin is coimmunoprecipitated only from extracts containing GFP:DallyΔgpi and CFP:DlpΔgpi, not secreted GFP.

(C and D) A single optical section 2 μm below the apical surface of a wing disc expressing GFP:Dlp ([D], green) in the dorsal compartment, stained with anti-Lipophorin (red). Lipophorin accumulates in Dlp-overexpressing cells. The epithelium curves down on the left of the image, bringing the disc lumen into focus there; the elevated staining in this region reflects Lipophorin in the lumen and not in the tissue itself.

(E and F) A single optical section 2 μm below the apical surface of a wing disc expressing GFP:Dally ([F], green) in the dorsal compartment, stained with anti-Lipophorin (red). Lipophorin accumulates in Dally-overexpressing cells. For both GFP:Dally- (C and D) and GFP:Dlp- (E and F) overexpressing cells, apical Lipophorin accumulation is sometimes associated with basal depletion of Lipophorin (data not shown).

(G and H) A wing disc expressing non-heparan-sulfate-modifiable GFP:DallyΔHS ([H], green) in the dorsal compartment stained with anti-Lipophorin (red). Lipophorin recruitment is heparan sulfate dependent.

(I and J) Basal surface of a wing disc with *ttv, botv* double-mutant clones marked by loss of GFP (I), stained for Lipophorin (J). Lipophorin is lost basally from *ttv, botv* mutant cells.

interact with low-density particles either through its gpi anchor or via HS (Figure 1E).

Most GFP:Dally released by imaginal disc cells cofractionates with Lipophorin particles with densities between 1.130 and 1.193 g/ml. Removal of the gpi anchor causes a shift to slightly higher densities (that still overlap those of Lipophorin particles). One explanation for this observation might be that HS-mediated interactions are less stable than those of the gpi anchor; dissociation of GFP:Dally from Lipophorin particles during centrifugation might strand non-gpi-anchored Dally in slightly higher density fractions. Alternatively, non-gpi-anchored Dally might not bind to Lipophorin but to some other low-density object. We therefore sought alternative approaches to investigate interactions between glypican heparan sulfate moieties and Lipophorin particles.

First, we asked whether Lipophorin particles could be coimmunoprecipitated with non-gpi-linked glypicans. While anti-GFP could not coimmunoprecipitate ApoLII from supernatants containing secreted GFP, it did so when supernatants contained either CFP:DallyΔgpi or GFP:DlpΔgpi (Figures 2A and 2B). These data show that glypicans specifically interact with Lipophorin particles independently of their gpi anchors.

Second, if glypicans bind Lipophorin via heparan sulfate, then membrane-associated glypicans should

recruit Lipophorin particles to imaginal disc cells. To test this prediction, we overexpressed either GFP:Dally or GFP:Dlp in the dorsal compartment of the wing disc and stained with antibodies to Lipophorin. Cells of the dorsal compartment clearly accumulate more Lipophorin than cells of the ventral compartment in both cases (Figures 2C–2F; quantified in Figure S1E). These data suggest glypicans indeed recruit Lipophorin particles. To examine whether HS was required for recruitment, we induced expression of GFP:DallyΔHS. Although GFP:DallyΔHS localized to the membrane as efficiently as GFP:Dally, and was expressed at equivalent levels, it did not recruit Lipophorin (Figures 2G and 2H; quantified in Figure S1E). These data show that membrane-associated glypicans recruit Lipophorin via their HS moieties—upon release from the membrane, glypicans may continue to interact with Lipophorin via HS.

To ask whether disc cells require HS to recruit Lipophorin particles, we examined Lipophorin distribution in clones mutant for the HS biosynthetic enzymes *tout-velu* (*ttv*) and *brother of tout-velu* (*botv*). Lipophorin accumulation was specifically reduced on the basal side of cells missing HS (Figures 2I and 2J, arrows), but was distributed normally in more apical regions (data not shown). Thus, HS is necessary for basal interaction of Lipophorin with disc cells, but multiple mechanisms probably mediate uptake of these important particles.

Released Dally Nonautonomously Rescues Reduced Growth of Dally Mutant Wings

We wondered whether the presence of released Dally on Lipophorin particles might alter their function. *dally* mutant wings have developmental defects, some of which may be caused by loss of membrane-associated Dally and others by loss of the released form. We presumed that Dally functions that depended on the membrane-associated form would cause autonomous defects in *dally* loss-of-function clones. Other, perhaps distinct, functions of released Dally would be rescued nonautonomously, and therefore impossible to identify in clones. The autonomous requirements for Dally in Wingless and Dpp signaling presumably reflect a requirement for the membrane-linked form in these processes (Belenkaya et al., 2004; Franch-Marro et al., 2005; Fujise et al., 2003; Han et al., 2005; Jackson et al., 1997; Kreuger et al., 2004; Lin and Perrimon, 1999; Tsuda et al., 1999). In addition to the loss of marginal bristles and defects in the fifth wing vein that results from Wg and Dpp signaling problems, Dally wings are smaller than those of wild-type (Figures 3A, 3B, and 3D), primarily due to a reduction in cell number, rather than cell size (Figure 3D). Both anterior and posterior compartments (Figure 3D), and all intervein regions, are affected (Figure S2A). To test whether this phenotype might be rescued nonautonomously, we expressed wild-type Dally in different subsets of the wing imaginal disc under the control of the GAL4UAS system. Expression of Dally in the posterior compartment of *dally* mutant discs increased the size of both the posterior and anterior compartments in the adult wing (Figures 3C and 3E). Furthermore, Dally overexpression in a wild-type background further increased the size of wild-type wings nonautonomously (Figure S2C). To test whether the nonautonomous growth caused by *dally* expression was due directly to the secreted form or to an indirect effect of membrane-anchored Dally, we asked whether it could be reproduced by expressing GFP:DallyΔgpi. When expressed in the posterior compartment of either wild-type or *dally* mutant wings, this secreted Dally isoform increased the size of the anterior compartment (Figures 3F and 3G). In contrast to wild-type Dally, the non-gpi-anchored form did not increase the size of the compartment where it was expressed (Figure 3G). Thus, released Dally directly and nonautonomously increases growth in the anterior, but not the posterior, compartment. Membrane-anchored Dally must autonomously promote posterior growth by a separate mechanism (Belenkaya et al., 2004; Takeo et al., 2005).

Dally Mutants Reduce the Range of Hh Target Gene Activation without Affecting Ci Stability

Because overexpression of secreted Dally in a wild-type background produced wing phenotypes similar to that of Hh overexpression (Figures 4A–4C) (Takeo et al., 2005), we wondered whether Hh signaling might be defective in *dally* mutant discs. Hh signaling activates long-range targets like *Dpp* by stabilizing the full-length transcriptional activator form of Cubitus interruptus (Ci) and promoting its translocation to the nucleus. Higher-level Hh signaling, which increases the activity but not the stability of Ci, is required for transcription of the short-range targets *engrailed* and *collier* (Kalderon, 2005; Lum and Beachy, 2004; Nybakken and Perrimon, 2002; Sisson et al., 2006; Wang et al., 2000; Wang and Holmgren, 1999, 2000). Quantitative immunostaining shows a highly significant reduction in the range of *engrailed*, *collier*, and *dpp* transcription in $dally^{80}$ mutant discs (Figures 4D–4F; Figures S3A–S3F). Despite this, the range of full-length Ci accumulation is normal (Figure 4J; Figures S4A and S4B); thus, Ci is stabilized normally but does not efficiently activate transcription in a *dally* mutant background.

To test whether Ci moved to the nucleus in *dally* mutant cells, we treated mutant discs with the nuclear export inhibitor Leptomycin B. Like wild-type discs (Sisson et al., 2006), *dally* mutant discs also accumulate nuclear Ci within 90 min after blocking nuclear export (Figures S4D, S4E, S4G, and S4H). Thus, nuclear translocation is normal but the presence of nuclear, full-length Ci is not sufficient to fully activate target gene transcription in a *dally* background. These data indicate Dally is required for Ci activation—the step requiring the highest level of Hh signaling.

Released Dally Rescues Hh Signaling in *dally* Mutant Discs

We wondered whether reduced Hh target gene activation in *dally* mutant wing discs, like reduced anterior growth, could be rescued by the released form. Expressing GFP:DallyΔgpi in the posterior compartment of $dally^{80}$ mutant discs extends the range of Engrailed and Collier

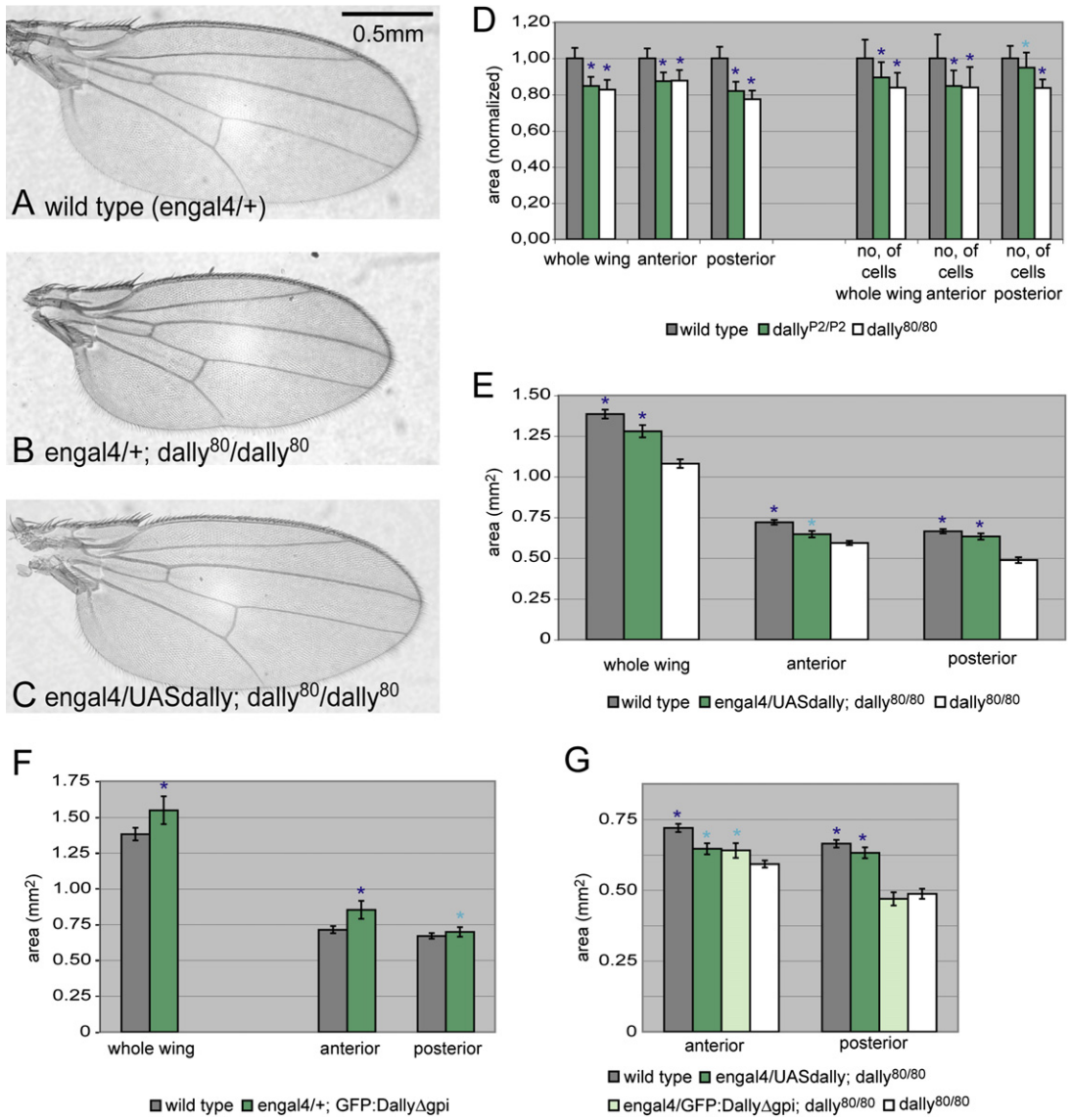

Figure 3. Released Dally Nonautonomously Rescues Growth of *dally*^{80}/*dally*^{80} Mutant Wings

Dark blue stars indicate p values < 0.01; light blue stars indicate p values < 0.05.

(A–C) Adult wings from *engal4*^{33}/+ (wild-type), *dally*^{80}/*dally*^{80}, and *engal4*^{33}/*UAS Dally; dally*^{80}/*dally*^{80} flies raised in parallel at identical temperature.

(D) Average wing size and cell number in anterior and posterior compartments of wild-type and *dally* mutants. *dally*^{80}/*dally*^{80} wings have fewer cells.

(E) Average wing size of *engal4*^{33}/+ (wild-type), *dally*^{80}/*dally*^{80}, and *engal4*^{33}/*UAS Dally; dally*^{80}/*dally*^{80} flies. Posterior Dally expression promotes growth of both anterior and posterior compartments.

(F) Average wing size of *engal4*^{33}/+ (wild-type) and *engal4*^{33}/*+; UAS:GFPDallyΔgpi*. Posteriorly secreted GFP:DallyΔgpi causes anterior overgrowth.

(G) Average wing size of *engal4*^{33}/+ (wild-type), *dally*^{80}/*dally*^{80}, *engal4*^{33}/*UAS Dally; dally*^{80}/*dally*^{80}, and *engal4*^{33}/*UAS:GFPDallyΔgpi; dally*^{80}/*dally*^{80}. Posteriorly secreted GFP:DallyΔgpi rescues only anterior growth.

Error bars indicate standard deviations.

production in the anterior compartment to equal that of wild-type (Figures 4E and 4F; Figures S3B, S3C, S3H, and S3I). Released Dally expression in *dally*^{80} mutant discs also broadens activation of the long-range target gene *Dpp*, even slightly beyond its normal range (Figure 4D; Figures S3A, S3D, and S3G). Thus, released Dally completely rescues all Hedgehog signaling defects in *dally* mutant wing discs.

Released Dally can also cause Hh gain-of-function phenotypes when overexpressed in a wild-type background. When overexpressed in the posterior compartment, released Dally extends the range of both *Dpp* activation and Ci stabilization beyond that of wild-type (Figures 4G and 4K; Figures S3A and S3J) (Takeo et al., 2005). However, it does not extend the activation of Collier or Engrailed beyond their normal range (Figures 4H and 4I;

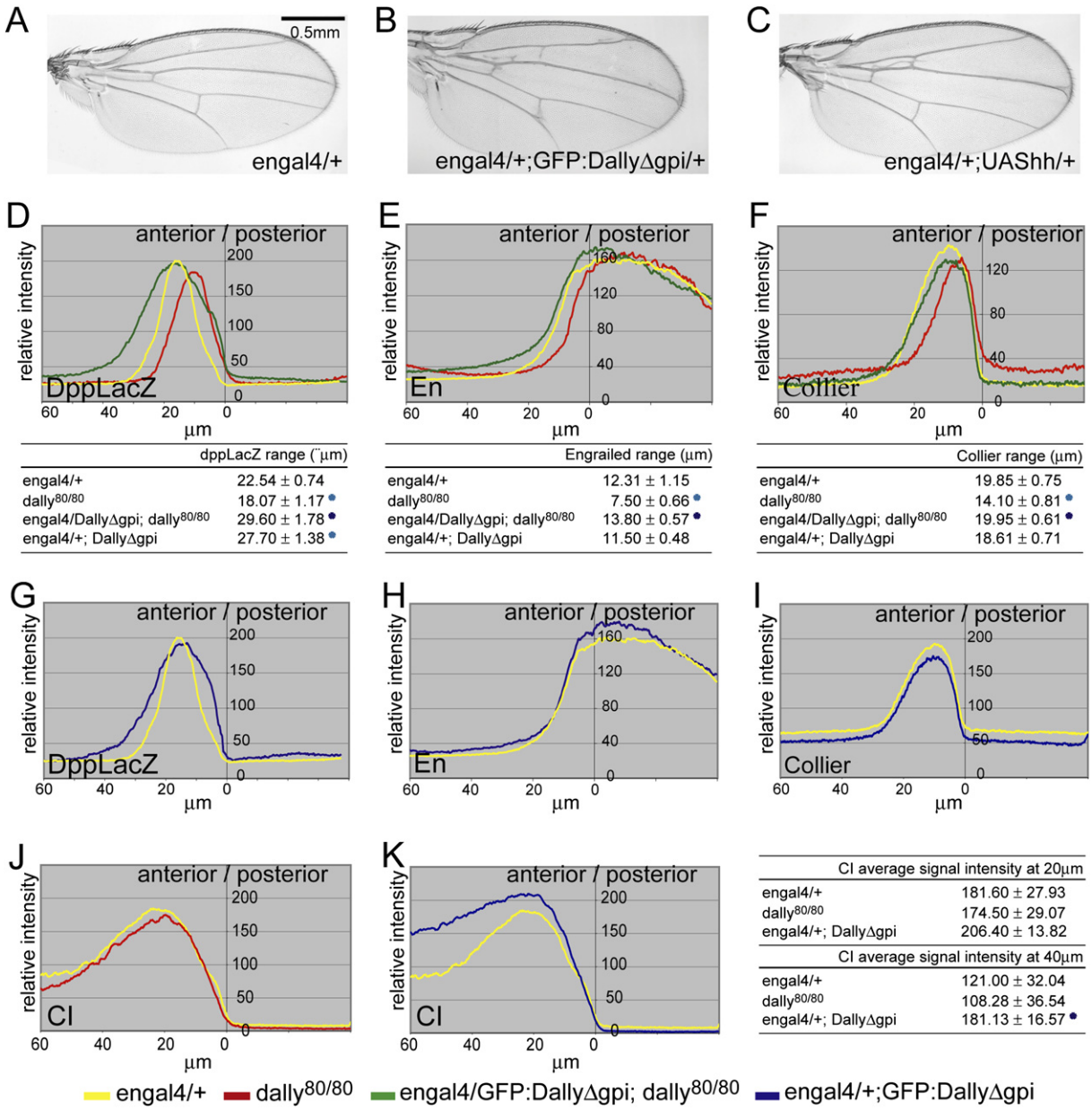

Figure 4. Full-Strength Hh Signaling Requires Released Dally

(A–C) Wings from wild-type *engal4*^{33}/+ (A), *engal4*^{33}/+; *GFP:Dally Δgpi*/+ (B), and *engal4*^{33}/+; *UAS:Hh*/+ (C) flies raised in parallel at identical temperature. Similar venation and overgrowth defects are caused by GFP:DallyΔgpi and Hh overexpression.

(D–F) Average Dpp (D), En (E), and Collier (F) staining intensity plotted against distance from the AP boundary in wild-type (yellow), *dally*^{80}/*dally*^{80} (red), and rescued (green) *engal4*^{33}/*UAS:GFPDally Δgpi; dally*^{80}/*dally*^{80} wing discs. Narrowed target gene activation in *dally* mutant discs is nonautonomously rescued by GFP:DallyΔgpi.

(D–I) Quantifications show average ± SD of the distance at which staining intensity is half-maximal. Stars indicate p values < 0.01. Light and dark blue indicate significant difference from wild-type or *dally*^{80} mutant, respectively.

(G–I) Average Dpp (G), En (H), and Collier (I) staining intensity in wild-type *engal4*^{33}/+ (yellow) and GFP:DallyΔgpi-overexpressing (blue) wing discs.

(J and K) Average staining intensity of full-length Ci plotted against distance from the AP boundary in wild-type (yellow), *dally*^{80}/*dally*^{80} (red), and *engal4*^{33}/*UAS:GFPDally Δgpi* (blue) wing discs. Ci range is normal in *dally*^{80}/*dally*^{80} discs, but can be extended by *GFP:Dally Δgpi* overexpression. Quantification shows average ± SD. Ci signal intensities are at different distances from the AP boundary. Blue star indicates significant ($p < 0.01$) extension of the range of Ci caused by *GFP:Dally Δgpi*.

(D–K) Between 6 and 16 discs were averaged in the experiments shown.

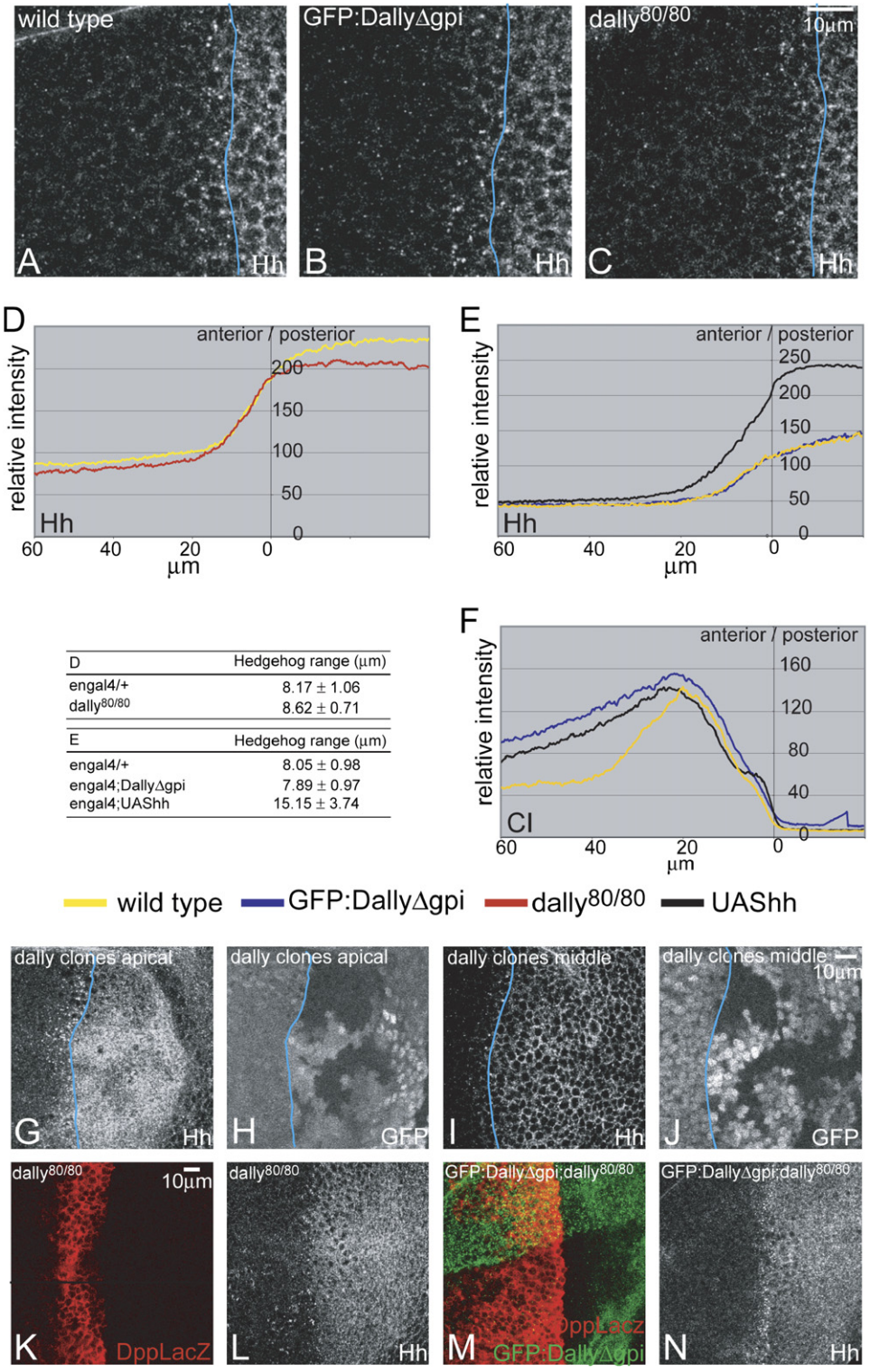

D	Hedgehog range (μm)
engal4/+	8.17 ± 1.06
dally$^{80/80}$	8.62 ± 0.71

E	Hedgehog range (μm)
engal4/+	8.05 ± 0.98
engal4;DallyΔgpi	7.89 ± 0.97
engal4;UAShh	15.15 ± 3.74

Figure 5. Released Dally Does Not Alter Hh Protein Levels in Receiving Tissue

(A–C) Wing discs from *engal4*^{33}/+ (wild-type) (A), GFP:DallyΔgpi-overexpressing (B), and *dally*^{80}/*dally*^{80} mutant (C) larvae stained with anti-Hh.

(D) Average Hh staining intensity with distance from the AP boundary from ten wild-type and ten *dally*^{80}/*dally*^{80} mutant discs. Hh distribution is not affected by *dally* mutation.

(E) Average Hh staining intensity with distance from the AP boundary of wild-type discs, or discs overexpressing either GFP:DallyΔgpi or Hh in the posterior compartment. GFP:DallyΔgpi overexpression does not extend the range of Hh in receiving tissue compared to wild-type. Hh overexpression dramatically increases Hh accumulation in receiving tissue.

Figures S3B, S3C, S3K, and S3L), suggesting that Hh signaling is already maximal in this region in wild-type discs.

We wondered whether released Dally needed to be expressed in posterior Hh-producing cells to extend the range of Hh signaling. To test this, we asked whether anterior expression (under the control of *ptcGAL4*) could activate target genes as efficiently as posterior expression. Released Dally causes a similar extension of Ci stability and *Dpp* transcription (Figures S5A–S5F) independently of its site of expression. Thus, released Dally need not be coexpressed with Hedgehog to exert its effects.

Released Dally Increases Hh Signaling without Affecting Hh Levels in Receiving Tissue

To test whether released Dally increased Hh signaling by affecting its spread or stability in receiving tissue, we quantified and compared Hh staining intensity in *dally* mutant and wild-type wing discs. The range and intensity of Hh staining in receiving tissue appears identical in these two genotypes (Figures 5A, 5C, and 5D). Thus, *dally* mutants accumulate normal levels of Hh in receiving cells.

Although *dally* mutant discs had apparently normal levels of Hh in receiving tissue, we wondered whether released Dally overexpression might be a more sensitive method to detect effects on Hh accumulation in this region. Therefore, we quantified Hedgehog staining in wild-type discs that overexpressed released Dally in the posterior compartment and compared them to that of wild-type (Figures 5A, 5B, and 5E). Hedgehog staining intensity in receiving tissue was indistinguishable in these two genotypes. To confirm that this method would have detected more Hedgehog if it had been there, we overexpressed Hedgehog in the posterior compartment to a level that extended Ci stability over a similar range as GFP:DallyΔgpi (Figure 5F). In this case, a dramatic increase in Hh accumulation in receiving cells was easily detected (Figure 5E). Thus, if GFP:DallyΔgpi had extended the range of Ci stabilization by increasing the level of Hh in receiving tissue, this assay would have been sensitive enough to detect it. These data confirm that released Dally is unlikely to act by increasing the amount of Hh in receiving tissue. Taken together, they show that GFP:DallyΔgpi increases the efficiency of Hh signaling without affecting spread or stability in receiving tissue.

Despite having normal levels of Hh in receiving tissue, *dally* mutant discs do appear to have mildly reduced levels of Hh in producing tissue (Figure 5D). To investigate whether this was caused by the released or membrane-associated form of Dally, we examined Hh staining in *dally* mutant clones. Apical Hh staining is modestly reduced in these cells (Figures 5G and 5H). The fact that it is reduced autonomously suggests that membrane-associated rather than released Dally is involved in Hh trafficking in producing cells.

To confirm that released Dally played no autonomous role in Hh trafficking in producing cells, we asked whether its expression in *dally* mutant discs could rescue Hh accumulation in producing tissue. Expression of released Dally in the dorsal compartment of *dally* mutant discs rescues the range of *dppLacZ* expression in both dorsal and ventral cells (compare Figures 5K and 5M), but has no effect whatsoever on Hh accumulation in producing cells (Figures 5L and 5N; Figure S6G). Overexpression in a wild-type background also increased signaling without autonomously changing Hh levels in producing cells (Figures S6H–S6M). Thus, the membrane-associated form, rather than the released form, is likely responsible for autonomously increasing Hh accumulation in producing cells. Because released Dally completely rescues Hh signaling without rescuing Hh accumulation in producing tissue, we conclude that altered Hh trafficking in producing tissue is not the primary cause of the signaling defects seen in *dally* mutant wing discs.

Our conclusions differ in some respects from those of a previous study, which argued that released Dally elevated Hh levels in receiving tissue when overexpressed (Takeo et al., 2005). This discrepancy may be attributable to the way that Hh was detected—the previous study relied on overexpressing Hh under the control of HhGAL4 to improve its visualization in receiving tissue, whereas we have quantified endogenous Hh staining. Takeo et al. (2005) also observe that released Dally autonomously decreases Hh levels in producing cells, whereas we do not observe any such change when GFP:DallyΔgpi is expressed. It is possible that different expression levels may account for the differences in our findings. However, because target gene activation occurs in both systems, whether Hh levels in producing cells are affected or not, it is likely that released Dally increases signaling independently of any effect on Hh in producing cells.

Released Dally and Hh Are Present on the Same Lipophorin Particles

The vast majority of both non-membrane-associated Hh and released Dally cofractionates with Lipophorin in biochemical assays (Panáková et al., 2005) (Figure 1). We therefore wondered whether the presence of both released Dally and Hh on the same particle might increase Hh signaling efficiency. To test whether released Dally and Hh were ever present on the same particles, we asked

(F) Average Ci staining intensity with distance from the AP boundary of wild-type discs, or discs overexpressing either GFP:DallyΔgpi or Hh in the posterior compartment. Despite the dramatic elevation of Hh in receiving tissue caused by Hh overexpression, the range of Ci stabilization is slightly less than that caused by GFP:DallyΔgpi.
(G–J) The apical (G and H) and middle (I and J) regions of a disc containing $dally^{80}$ mutant clones, marked by loss of GFP (H) and stained for Hh (G).
(K and L) $dally^{80}$ homozygous mutant disc stained for Hh (L) and DppLacZ ([K], red).
(M and N) $dally^{80}$ homozygous mutant disc rescued by GFP:DallyΔgpi expression in the dorsal compartment stained for DppLacZ ([M], red), GFP ([M], green), and Hh (N).

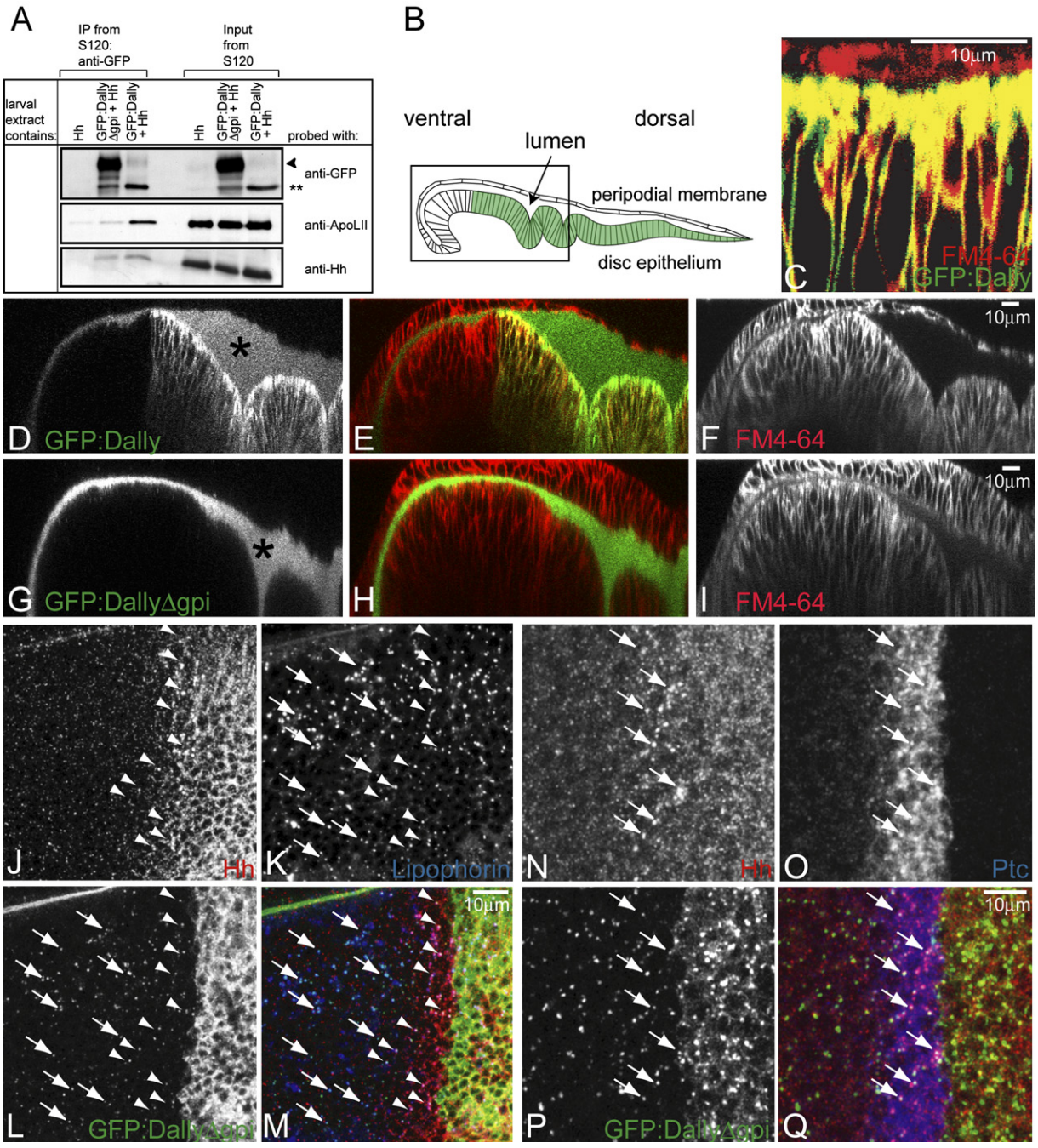

Figure 6. Released Dally, Lipophorin, and Hh Interact and Colocalize

(A) S120s from larvae expressing either Hh alone, Hh+GFP:Dally, or Hh+GFP:DallyΔgpi in posterior disc compartments, precipitated with anti-GFP and probed with either anti-GFP, anti-Hh, or anti-ApoLII. Arrowheads indicate full-length GFP:Dally and GFP:DallyΔgpi; asterisks indicate the released N-terminal fragment. Anti-GFP precipitates GFP:Dally and GFP:DallyΔgpi from S120s, along with both Hh and Lipophorin. Full-length GFP:DallyΔgpi coprecipitates both Hh and Lipophorin less efficiently than GFP:Dally, possibly reflecting its less stable association with Lipophorin, or differences in its mode of formation.

(B) Cartoon of the sections shown in (D)–(I).

(C) XZ section of a wing disc expressing GFP:Dally stained for FM4-64. GFP:Dally localizes to membranes.

(D–F) XZ section of a living wing disc expressing GFP:Dally ([D and E], green) stained with FM4-64 ([F and E], red). GFP:Dally is present on expressing cell membranes and is secreted into the apical lumen (asterisk).

(G–I) XZ section of a living wing disc expressing GFP:DallyΔgpi ([G and H], green) in the dorsal compartment stained with FM4-64 ([H and I], red). GFP:DallyΔgpi is secreted into the lumen (asterisk).

whether antibodies to GFP:Dally could precipitate Hh as well as Lipophorin from S120s of larval extracts (Figure 6A). Anti-GFP precipitated both Lipophorin and Hh when S120s were prepared from larvae in which either GFP:Dally or GFP:DallyΔgpi were expressed in imaginal discs. No Hh was precipitated by anti-GFP from S120s that did not contain either GFP:Dally or GFP:DallyΔgpi. Thus, at least a fraction of released Dally and Hh are present on the same Lipophorin particles.

To confirm the association of Lipophorin, Hh, and released Dally in vivo, we examined their localization in wing imaginal discs. GFP:Dally, which produces both membrane-linked and released forms of the protein, is detected both on plasma membranes of expressing cells and within the apical lumen of the disc (Figures 6B–6F). Non-membrane-anchorable GFP:DallyΔgpi is detected in the apical lumen and within endosomes of receiving cells (Figures 6G–6I; Figures S7A, S7B, S7E, and S7F). Thus, gpi linkage targets GFP:Dally to the membrane, whereas the non-lipid-modified form is apically secreted and internalized.

GFP:DallyΔgpi colocalizes extensively with Lipophorin, Hh, and Ptc in the endosomes of receiving tissue (Figures 6J–6Q; Figure S7). Seventy-seven percent ± 1% of Hh-positive endosomes and 86% ± 8% of endosomes containing GFP:DallyΔgpi also contain Lipophorin. Of those endosomes containing both Hh and Lipophorin, 53% ± 21% were also positive for GFP:DallyΔgpi (Figures 6J–6M, arrowheads). We also observe frequent triple colocalization between Hh, GFP:DallyΔgpi, and Ptc (Figures 6N–6Q, arrows). These data confirm the physical interactions detected between GFP:DallyΔgpi, Hh, and Lipophorin in biochemical assays, and suggest that most GFP:DallyΔgpi is internalized with Lipophorin particles throughout the disc epithelium. In Hh receiving tissue, GFP:DallyΔgpi is present in the same endosomes with Hh, Lipophorin, and Ptc.

Rab5-Dependent Endocytosis Internalizes Hh, Ptc, and Lipophorin from Separate Apical and Basal Pools

Although these data suggest that Lipophorin particles containing both released Dally and Hedgehog are internalized by imaginal disc cells, we were puzzled as to how and where these proteins could encounter each other. GFP:DallyΔgpi is present in the apical lumen, whereas Lipophorin is derived basally from the hemolymph. Furthermore, while it is clear that Hh is internalized basolaterally, it is controversial whether any fraction of Hh is secreted to the apical side of the disc epithelium (Callejo et al., 2006; Gallet et al., 2006; Han et al., 2005). This led us to wonder whether these proteins might converge in endosomes after internalization from separate apical and basal surfaces. Alternatively, if disc cells do directly internalize Lipophorin particles containing both GFP:DallyΔgpi and Hedgehog, then at least a fraction of Hedgehog and Lipophorin must be present in the apical lumen with GFP:DallyΔgpi. To test whether any fraction of Lipophorin or Hedgehog was present apical to disc epithelial cells, we used short-term expression of dominant-negative Rab5 (Rab5SN) to block endocytosis (Marois et al., 2006) and trap these proteins on the surfaces from which they are internalized. Five hours after initiating Rab5SN expression in the dorsal compartment, we stained discs for Ptc, Hh, and Lipophorin and compared their localization in wild-type and Rab5SN-expressing halves of the wing pouch (Figure 7, brackets).

Interestingly, Lipophorin levels increase on apical and basal, but not lateral, surfaces when endocytosis is blocked (Figures 7M–7O). The fact that a fraction of Lipophorin is internalized apically suggests that hemolymph-derived Lipophorin particles arriving basally may be transcytosed and resecreted into the apical lumen where released Dally is also present.

Hh and Ptc also accumulate both apically and (more strongly) basally in receiving tissue when endocytosis is blocked (Figures 7A, 7C, 7D, and 7F–7L; Figure S8). Rab5SN expression does not cause either protein to accumulate in lateral regions of disc epithelial cells (Figures 7B and 7E). These data suggest that Hedgehog is secreted into both apical and basal pools and internalized from the apical and basal sides of receiving cells—with basal uptake predominating. Thus, Lipophorin particles bearing both Hh and GFP:DallyΔgpi may be present in the apical lumen and internalized from the apical surface. We hypothesize that the presence of released Dally on these particles increases Hh signaling at the apical surface, possibly by forming part of a signaling complex with Ptc.

DISCUSSION

The mechanisms that control the spread and activity of Hh are critical regulators of pattern formation and growth. Hh is modified by both cholesterol and palmitate—in addition to conferring membrane affinity and limiting the spread of the protein, these modifications are essential for normal signaling activity (Callejo et al., 2006; Chamoun et al., 2001; Gallet et al., 2003, 2006; Lewis et al., 2001; Pepinsky et al., 1998; Porter et al., 1996; Willert et al., 2003). We have recently shown that lipid-modified Hh can be released from the plasma membrane on lipoprotein particles and that this association is essential for long-range signaling. Both Hh trafficking and signaling also depend on heparan sulfate proteoglycans (Han et al., 2004a; Takei et al., 2004; The et al., 1999)—in particular the glypicans

(J–M) Single confocal section of a wing disc expressing GFP:DallyΔgpi ([L and M], green) in the posterior compartment, stained for Hedgehog ([J and M], red) and Lipophorin ([K and M], blue). Arrowheads indicate triple colocalization between Lipophorin, GFP:DallyΔgpi, and Hh. Arrows indicate double colocalization between Lipophorin and GFP:DallyΔgpi.
(N–Q) Single confocal section of a wing disc expressing GFP:DallyΔgpi ([P and Q], green) in the posterior compartment, stained for Hh ([N and Q], red) and Ptc ([O and Q], blue). Arrows indicate colocalization.

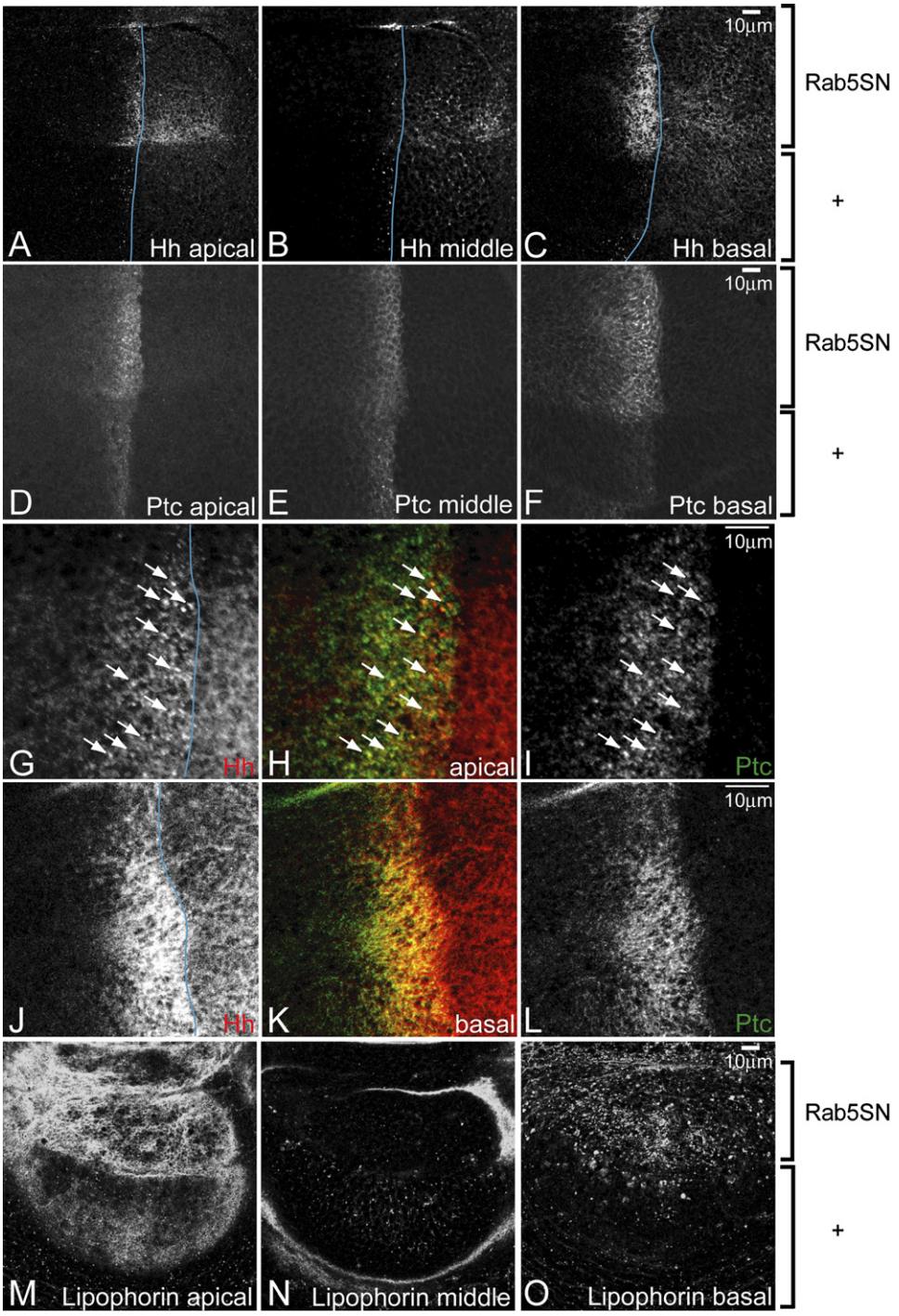

Figure 7. Ptc, Hh, and Lipophorin Are Internalized from Apical and Basal but Not Lateral Surfaces

In (A)–(L), a blue line separates posterior Hh producing cells (right) from anterior Hh receiving cells (left).

(A–F) Projections of four 0.5 μm confocal sections through apical (A and D), middle (B and E), and basal (C and F) regions of two different wing discs 5 hr 30 min after inducing Rab5SN expression in the dorsal compartment by excision of an intervening HcRed cassette. The discs were stained with either anti-Hh (A–C) or anti-Ptc (D–F), detected with an Alexa 488-conjugated secondary antibody. Brackets indicate Rab5SN-expressing region and wild-type (+) region. Separately stained discs are shown to avoid faint residual HcRed emission, which overlaps that of Cy5. In receiving cells, Hh and Ptc accumulate on apical and basal surfaces of Rab5SN-expressing tissue. In posterior Hh secreting cells, blocking Rab5-dependent endocytosis causes apical Hh accumulation, consistent with a previous study (Callejo et al., 2006).

(G–L) Higher-magnification view of Ptc (I and L) ([H and K], green) and Hh (G and J) ([H and K], red) accumulation in Rab5SN-expressing cells in double-stained discs. Accumulated Hh protein is detected above the faint background of HcRed. Apical (G–I) and basal (J–L) surfaces are shown. Arrows indicate apical Hh-Ptc colocalization. Basal colocalization is almost absolute.

Dally and Dlp (Han et al., 2004b). The cell biological mechanisms by which HSPGs control Hh spread and signaling are unknown. Here we have examined the relationship between glypicans and Lipophorin in the Hh pathway.

Lipophorin Interacts with Glypicans via Heparan Sulfate

We have established that Lipophorin particles bind to the heparan sulfate moieties of glypicans. One consequence of this is that membrane-associated Dally and Dlp can recruit Lipophorin particles to imaginal disc tissue. Indeed, HSPGs are autonomously required for Lipophorin's interaction with the basal side of the disc epithelium. This raises the possibility that HSPGs may recruit lipid-linked morphogens to receiving cells, at least in part, by binding to morphogen-bearing lipoprotein particles. Although Hh is present in both apical and basal pools in the wing disc, it accumulates much more strongly on the basal surface when endocytosis is blocked. This suggests that the majority of Hh protein may spread along the basal surface. *ttv, botv* mutant cells that cannot recruit Lipophorin basally may be compromised in their ability to interact with Hh-bearing Lipophorin particles. This idea is also consistent with the observation that Hh mutants that cannot be sterol modified (and are presumably not associated with lipoproteins) no longer depend on HSPGs to bind to receiving cells (The et al., 1999).

Our data suggest that Lipophorin must be transcytosed from the basal side of the disc to the apical lumen. Although membrane-associated Dally and Dlp are found on the basolateral membrane, removal of the gpi anchor results in apical secretion. It will be interesting to investigate whether glypican endocytosis and subsequent release might play a role in Lipophorin transcytosis. The presence of transcytosed particles in the disc lumen may explain why removal of HS from clones of cells only disrupts basal Lipophorin accumulation. Particles transcytosed by other cells would be available for apical internalization by HS-independent mechanisms.

Dally and Dlp continue to associate with Lipophorin via HS moieties after cleavage of the gpi anchor. The fact that both glypicans remain bound to Lipophorin after shedding raises the possibility that released glypicans influence signaling from lipoprotein particles. Our analysis of the role of released Dally supports this idea.

Released Dally Increases Hh Signaling Efficiency but Not Spreading

Our data indicate that released Dally is required for full-strength Hh signaling, but does not affect the range over which Hh spreads. Hh signaling promotes Ci-dependent target gene activation by three separable mechanisms that are differentially sensitive to Hh levels. Ci stabilization requires the lowest levels of Hh signaling, and thus occurs over the broadest range. Ci stabilization is insufficient for target gene activation, however (Methot and Basler, 1999; Wang and Holmgren, 1999). To activate transcription, full-length Ci must be released with Suppressor of Fused (Su[Fu]) from cytoplasmic complexes containing Fused and Costal-2 and translocate to the nucleus. This occurs over shorter distances than Ci stabilization. Still higher levels of Hh signaling induce other processes needed for full activity of the Ci-Su(Fu) heterodimer within the nucleus (Kalderon, 2005; Lum and Beachy, 2004; Nybakken and Perrimon, 2002; Sisson et al., 2006; Wang et al., 2000; Wang and Holmgren, 1999, 2000). These are less well understood, but may involve phosphorylation of Su(Fu) (Ho et al., 2005). In *dally* mutant discs, Ci stabilization and nuclear translocation, which require lower levels of Hh signaling, are normal. Only Ci activation is impaired by loss of *dally*. Thus, released Dally appears to increase the quantitative output of the Hh signaling pathway without increasing the amount of Hh.

Although we cannot rule out the possibility that a small, non-particle-associated fraction of released Dally gives rise to the phenotypes we see, the extensive cofractionation and colocalization of released Dally with Lipophorin suggests that it may act by influencing the behavior of these particles. For example, interaction of Lipophorin with the HS moieties of released Dally might reduce the affinity of Lipophorin particles for cell-surface HS, promoting transfer of Hh-bearing particles to Ptc. Alternatively, Dally HS moieties on Hh-bearing lipoprotein particles might promote the formation of ligand-receptor complexes. IHog acts as a coreceptor with Ptc and, like released Dally, is necessary for full-strength Hh signaling (Yao et al., 2006). Adding soluble heparin induces IHog dimerization and increases IHog-Hh binding in vitro (McLellan et al., 2006). Presentation of Dally HS on the same particle with Hh may greatly increase the efficiency with which these complexes form by bringing HS, Hh, and IHog into close proximity in vivo. Furthermore, lipoprotein particles that carried multiple copies of Dally and Hh would have the potential to induce receptor crosslinking. In this way, lipoprotein particles may act as scaffolding platforms, bringing together specific ligands and increasing the diversity of combinatorial signals available for patterning during development.

EXPERIMENTAL PROCEDURES

Fly Stocks

The wild-type Oregon R, *apGal4*, *ptcGal4*, *hs-flp*, *dally*^{P2}, *hh*^{ts}, and *dppLacZ* fly stocks are available from the Bloomington Stock Center. *enGal4*^{33} flies were a gift from Christian Dahmann. This line remains restricted to the posterior compartment in late third instar discs and does not reflect the Hh-driven engrailed expression on the anterior side of the boundary (C. Dahmann, personal communication). *dally*^{80} flies were from Xinhua Lin. Transgenic lines: *UAS:secretedGFP* (Entchev et al., 2000); *UAS:hh* (Bloomington); *UAS:GFP:CD63*

(M–O) Apical (M), middle (N), and basal (O) confocal sections of a wing disc stained for Lipophorin 5 hr 30 min after inducing Rab5SN expression in the dorsal compartment (brackets). Lipophorin accumulates apically and basally, not laterally, in Rab5SN-expressing regions compared to wild-type.

(Panáková et al., 2005); *UAS < hcRed > Rab5SN*, *UAS < hcRed > Rab7SN*, *tubP:CFP:Rab5*, and *tubP:YFPRab7* (Marois et al., 2006).

Construction of Tagged and Mutant Glypican Isoforms

GFP:Dally and *CFP:Dally* were constructed in p*UAST* by generating an NcoI site between nucleotides 173 and 178 and inserting either GFP or CFP with NcoI linkers. GFP is inserted shortly after the signal sequence with the concomitant deletion of lysine 58.

p*UAST:GFP:Dally*Δ*gpi* was constructed from p*UAST:GFP:Dally* by converting asparagine 604 to a stop codon.

p*UAST:GFP:Dally*Δ*HS* was constructed from p*UAST:GFP:Dally* by mutating serines 549, 569, and 573 to alanines.

To construct *UAS:GFPdlp* and *UAS:YFPDlp*, we cloned GFP or YFP with SphI linkers into an introduced SphI site shortly after the signal sequence, replacing glycine 69 with cysteine.

*UAS:GFPDlp*Δ*gpi* was made by changing arginine 743 to a stop codon.

Fractionation

Homogenization and centrifugation to obtain the 120,000 × g pellet (P120) and supernatant (S120), and fractionation of S120 in KBr isopycnic density gradients, were performed as described (Panáková et al., 2005).

For Optiprep (Axishield) gradients, the S120 from 50 larvae was mixed and adjusted to 50% Optiprep. Solutions of 10%–20% to 35%–45% Optiprep were layered on top of the sample and centrifuged at 4°C for 16 hr at 50,000 rpm (285,000 × g) in a TLS55 rotor (Beckman).

Drug Treatment

PI-PLC treatment was performed as described (Marois et al., 2006). Leptomycin B (20 nM; Sigma) was added to discs at 29°C for 90 min before fixation.

Immunoprecipitation

S120s from larvae expressing *UAS:secretedGFP*, *UAS:GPFDally*Δ*gpi*, or *UAS:CFPDlp*Δ*gpi* were precleared with protein G Sepharose 4 Fast Flow (Amersham) beads, then incubated overnight at 4°C with beads linked to mouse anti-GFP(106A20) (produced by the antibody facility of the MPI-CBG, Dresden). Beads were washed ten times in PBS and eluted with Laemmle buffer.

Antibodies

For western blotting: mouse anti-GFP, 1:750 (Santa Cruz); anti-ApoLII, 1:1000 (Panáková et al., 2005); secondary HRP-conjugated antibodies (Dianova, Jackson), 1:3000.

New anti-Lipophorin sera were generated by immunizing rabbits (MPI-CBG Antibody Facility, Dresden) or guinea pigs (Eurogentec, Seraing, Belgium) with larval lipoproteins purified on a KBr gradient and desalted on NAP columns (Amersham). Antisera detected primarily ApoLI and ApoLII on western blots, and signals were strongly reduced by anti-Lipophorin RNAi (Figure S9).

To produce anti-Hh, we immunized rabbits with Hh amino acids 90–471 fused to an N-terminal His tag. Antiserum was affinity purified against Hh amino acids 82–257 fused to GST.

Immunostaining and Microscopy

Immunostaining was performed as described (Strigini and Cohen, 2000). Zenon reagent (Molecular Probes) was used as recommended to label primary antibodies for use with antibodies from the same organism. Live imaging of imaginal discs was performed as described (Greco et al., 2001). Images were collected with a Leica TCS SP2 or a Zeiss LSM 510 confocal microscope.

Image Analysis

To quantify immunostaining intensity of Hh and its targets, discs were dissected, fixed, and stained in parallel and imaged under identical conditions. ImageJ was used to quantify the range and intensity of gene expression in five projected sections of Hh, Ci, En, Col, and DpplacZ-stained discs. For each image, we selected a 400 by 300 pixel rectangle centered around the anterior-posterior (AP) boundary and used the Plot Profile function of ImageJ to calculate the average pixel intensity as a function of distance from the AP boundary. These values were averaged for at least six different discs and plotted using Microsoft Excel.

Colocalization between Hh, Lipophorin, and Dally was quantified as described (Marois et al., 2006).

Images of adult wings were generated using a 5× or 10× objective with a Zeiss Axioplan microscope. ImageJ was used to select and measure the area of each intervein region. At least ten wings were analyzed per genotype. The area of the anterior compartment was defined as the combined areas of intervein regions between L1, L2, L3, and L4. The posterior compartment area was the sum of areas between L4, L5, and the posterior wing margin.

To determine the average cell size in different regions of the wing, we counted the number of wing hairs within a square of defined area and divided the area of the square by the number of hairs. As an estimate of cell number in a specific intervein region or compartment, we divided the area of the region by the average cell size in that region.

Supplemental Data

Supplemental Data include nine figures and are available at http://www.developmentalcell.com/cgi/content/full/13/1/57/DC1/.

ACKNOWLEDGMENTS

We gratefully acknowledge Isabel Guerrero, Robert Holmgren, Tadashi Uemura, Alain Vincent, and the MPI-CBG Antibody Facility for providing antibodies. We thank the MPI-CBG Light Microscopy Facility for microscopy support. We are grateful to Marino Zerial, Annette Schenck, and Christian Dahmann for critical comments on the manuscript. D.P. was supported by the Max Planck Gesellschaft and by a grant from the Deutsche Forschungsgemeinschaft (DFG) (4/2-1). C.E. was supported by DFG SPP 1111.

Received: November 24, 2006
Revised: March 27, 2007
Accepted: April 26, 2007
Published: July 2, 2007

REFERENCES

Ashe, H.L. (2005). BMP signalling: synergy and feedback create a step gradient. Curr. Biol. *15*, R375–R377.

Ashe, H.L., and Briscoe, J. (2006). The interpretation of morphogen gradients. Development *133*, 385–394.

Baeg, G.H., Selva, E.M., Goodman, R.M., Dasgupta, R., and Perrimon, N. (2004). The Wingless morphogen gradient is established by the cooperative action of Frizzled and heparan sulfate proteoglycan receptors. Dev. Biol. *276*, 89–100.

Belenkaya, T.Y., Han, C., Yan, D., Opoka, R.J., Khodoun, M., Liu, H., and Lin, X. (2004). *Drosophila* Dpp morphogen movement is independent of dynamin-mediated endocytosis but regulated by the glypican members of heparan sulfate proteoglycans. Cell *119*, 231–244.

Callejo, A., Torroja, C., Quijada, L., and Guerrero, I. (2006). Hedgehog lipid modifications are required for Hedgehog stabilization in the extracellular matrix. Development *133*, 471–483.

Chamoun, Z., Mann, R.K., Nellen, D., von Kessler, D.P., Bellotto, M., Beachy, P.A., and Basler, K. (2001). Skinny hedgehog, an acyltransferase required for palmitoylation and activity of the hedgehog signal. Science *293*, 2080–2084.

Day, S.J., and Lawrence, P.A. (2000). Measuring dimensions: the regulation of size and shape. Development *127*, 2977–2987.

De Cat, B., Muyldermans, S.Y., Coomans, C., Degeest, G., Vanderschueren, B., Creemers, J., Biemar, F., Peers, B., and David, G.

(2003). Processing by proprotein convertases is required for glypican-3 modulation of cell survival, Wnt signaling, and gastrulation movements. J. Cell Biol. *163*, 625–635.

Eaton, S. (2006). Release and trafficking of lipid-linked morphogens. Curr. Opin. Genet. Dev. *16*, 17–22.

Entchev, E.V., Schwabedissen, A., and Gonzalez-Gaitan, M. (2000). Gradient formation of the TGF-β homolog Dpp. Cell *103*, 981–991.

Franch-Marro, X., Marchand, O., Piddini, E., Ricardo, S., Alexandre, C., and Vincent, J.P. (2005). Glypicans shunt the Wingless signal between local signalling and further transport. Development *132*, 659–666.

Fujise, M., Takeo, S., Kamimura, K., Matsuo, T., Aigaki, T., Izumi, S., and Nakato, H. (2003). Dally regulates Dpp morphogen gradient formation in the *Drosophila* wing. Development *130*, 1515–1522.

Gallet, A., Rodriguez, R., Ruel, L., and Therond, P.P. (2003). Cholesterol modification of hedgehog is required for trafficking and movement, revealing an asymmetric cellular response to hedgehog. Dev. Cell *4*, 191–204.

Gallet, A., Ruel, L., Staccini-Lavenant, L., and Therond, P.P. (2006). Cholesterol modification is necessary for controlled planar long-range activity of Hedgehog in *Drosophila* epithelia. Development *133*, 407–418.

Greco, V., Hannus, M., and Eaton, S. (2001). Argosomes: a potential vehicle for the spread of morphogens through epithelia. Cell *106*, 633–645.

Gurdon, J.B., and Bourillot, P.Y. (2001). Morphogen gradient interpretation. Nature *413*, 797–803.

Han, C., Belenkaya, T.Y., Khodoun, M., Tauchi, M., Lin, X., and Lin, X. (2004a). Distinct and collaborative roles of *Drosophila* EXT family proteins in morphogen signalling and gradient formation. Development *131*, 1563–1575.

Han, C., Belenkaya, T.Y., Wang, B., and Lin, X. (2004b). *Drosophila* glypicans control the cell-to-cell movement of Hedgehog by a dynamin-independent process. Development *131*, 601–611.

Han, C., Yan, D., Belenkaya, T.Y., and Lin, X. (2005). *Drosophila* glypicans Dally and Dally-like shape the extracellular Wingless morphogen gradient in the wing disc. Development *132*, 667–679.

Ho, K.S., Suyama, K., Fish, M., and Scott, M.P. (2005). Differential regulation of Hedgehog target gene transcription by Costal2 and Suppressor of Fused. Development *132*, 1401–1412.

Jackson, S.M., Nakato, H., Sugiura, M., Jannuzi, A., Oakes, R., Kaluza, V., Golden, C., and Selleck, S.B. (1997). dally, a *Drosophila* glypican, controls cellular responses to the TGF-β-related morphogen, Dpp. Development *124*, 4113–4120.

Kalderon, D. (2005). The mechanism of hedgehog signal transduction. Biochem. Soc. Trans. *33*, 1509–1512.

Kolset, S.O., and Salmivirta, M. (1999). Cell surface heparan sulfate proteoglycans and lipoprotein metabolism. Cell. Mol. Life Sci. *56*, 857–870.

Kreuger, J., Perez, L., Giraldez, A.J., and Cohen, S.M. (2004). Opposing activities of Dally-like glypican at high and low levels of Wingless morphogen activity. Dev. Cell *7*, 503–512.

Lewis, P.M., Dunn, M.P., McMahon, J.A., Logan, M., Martin, J.F., St-Jacques, B., and McMahon, A.P. (2001). Cholesterol modification of sonic hedgehog is required for long-range signaling activity and effective modulation of signaling by Ptc1. Cell *105*, 599–612.

Lin, X., and Perrimon, N. (1999). Dally cooperates with *Drosophila* Frizzled 2 to transduce Wingless signalling. Nature *400*, 281–284.

Lum, L., and Beachy, P.A. (2004). The Hedgehog response network: sensors, switches, and routers. Science *304*, 1755–1759.

Marois, E., Mahmoud, A., and Eaton, S. (2006). The endocytic pathway and formation of the Wingless morphogen gradient. Development *133*, 307–317.

McLellan, J.S., Yao, S., Zheng, X., Geisbrecht, B.V., Ghirlando, R., Beachy, P.A., and Leahy, D.J. (2006). Structure of a heparin-dependent complex of Hedgehog and Ihog. Proc. Natl. Acad. Sci. USA *103*, 17208–17213.

Methot, N., and Basler, K. (1999). Hedgehog controls limb development by regulating the activities of distinct transcriptional activator and repressor forms of Cubitus interruptus. Cell *96*, 819–831.

Nybakken, K., and Perrimon, N. (2002). Hedgehog signal transduction: recent findings. Curr. Opin. Genet. Dev. *12*, 503–511.

Panáková, D., Sprong, H., Marois, E., Thiele, C., and Eaton, S. (2005). Lipoprotein particles are required for Hedgehog and Wingless signalling. Nature *435*, 58–65.

Pepinsky, R.B., Zeng, C., Wen, D., Rayhorn, P., Baker, D.P., Williams, K.P., Bixler, S.A., Ambrose, C.M., Garber, E.A., Miatkowski, K., et al. (1998). Identification of a palmitic acid-modified form of human Sonic hedgehog. J. Biol. Chem. *273*, 14037–14045.

Porter, J.A., Young, K.E., and Beachy, P.A. (1996). Cholesterol modification of Hedgehog signaling proteins in animal development. Science *274*, 255–259.

Ruiz i Altaba, A., Nguyen, V., and Palma, V. (2003). The emergent design of the neural tube: prepattern, SHH morphogen and GLI code. Curr. Opin. Genet. Dev. *13*, 513–521.

Sisson, B.E., Ziegenhorn, S.L., and Holmgren, R.A. (2006). Regulation of Ci and Su(fu) nuclear import in *Drosophila*. Dev. Biol. *294*, 258–270.

Strigini, M., and Cohen, S.M. (2000). Wingless gradient formation in the *Drosophila* wing. Curr. Biol. *10*, 293–300.

Takei, Y., Ozawa, Y., Sato, M., Watanabe, A., and Tabata, T. (2004). Three *Drosophila* EXT genes shape morphogen gradients through synthesis of heparan sulfate proteoglycans. Development *131*, 73–82.

Takeo, S., Akiyama, T., Firkus, C., Aigaki, T., and Nakato, H. (2005). Expression of a secreted form of Dally, a *Drosophila* glypican, induces overgrowth phenotype by affecting action range of Hedgehog. Dev. Biol. *284*, 204–218.

The, I., Bellaiche, Y., and Perrimon, N. (1999). Hedgehog movement is regulated through tout velu-dependent synthesis of a heparan sulfate proteoglycan. Mol. Cell *4*, 633–639.

Tsuda, M., Kamimura, K., Nakato, H., Archer, M., Staatz, W., Fox, B., Humphrey, M., Olson, S., Futch, T., Kaluza, V., et al. (1999). The cell-surface proteoglycan Dally regulates Wingless signalling in *Drosophila*. Nature *400*, 276–280.

Vincent, J.P., and Dubois, L. (2002). Morphogen transport along epithelia, an integrated trafficking problem. Dev. Cell *3*, 615–623.

Wang, Q.T., and Holmgren, R.A. (1999). The subcellular localization and activity of *Drosophila* cubitus interruptus are regulated at multiple levels. Development *126*, 5097–5106.

Wang, Q.T., and Holmgren, R.A. (2000). Nuclear import of cubitus interruptus is regulated by hedgehog via a mechanism distinct from Ci stabilization and Ci activation. Development *127*, 3131–3139.

Wang, G., Amanai, K., Wang, B., and Jiang, J. (2000). Interactions with Costal2 and suppressor of fused regulate nuclear translocation and activity of cubitus interruptus. Genes Dev. *14*, 2893–2905.

Willert, K., Brown, J.D., Danenberg, E., Duncan, A.W., Weissman, I.L., Reya, T., Yates, J.R., III, and Nusse, R. (2003). Wnt proteins are lipid-modified and can act as stem cell growth factors. Nature *423*, 448–452.

Wilsie, L.C., and Orlando, R.A. (2003). The low density lipoprotein receptor-related protein complexes with cell surface heparan sulfate proteoglycans to regulate proteoglycan-mediated lipoprotein catabolism. J. Biol. Chem. *278*, 15758–15764.

Wilsie, L.C., Chanchani, S., Navaratna, D., and Orlando, R.A. (2005). Cell surface heparan sulfate proteoglycans contribute to intracellular lipid accumulation in adipocytes. Lipids Health Dis. *4*, 2.

Yao, S., Lum, L., and Beachy, P. (2006). The ihog cell-surface proteins bind Hedgehog and mediate pathway activation. Cell *125*, 343–357.